ORIGINAL ARTICLE

[11C]5-HTP and microPET are not suitable for pharmacodynamic studies in the rodent brain

Anniek KD Visser[1], Nisha K Ramakrishnan[1], Antoon TM Willemsen[1], Valentina Di Gialleonardo[1], Erik FJ de Vries[1], Ido P Kema[2], Rudi AJO Dierckx[1] and Aren van Waarde[1]

The PET tracer [11C]5-hydroxytryptophan ([11C]5-HTP), which is converted to [11C]5-hydroxytryptamine ([11C]5-HT) by aromatic amino acid decarboxylase (AADC), is thought to measure 5-HT synthesis rates. But can we measure these synthesis rates by kinetic modeling of [11C]5-HTP in rat? Male rats were scanned with [11C]5-HTP (60 minutes) after different treatments. Scans included arterial blood sampling and metabolite analysis. 5-HT synthesis rates were calculated by a two-tissue compartment model (2TCM) with irreversible tracer trapping or Patlak analysis. Carbidopa (inhibitor peripheral AADC) dose-dependently increased [11C]5-HTP brain uptake, but did not influence 2TCM parameters. Therefore, 10 mg/kg carbidopa was applied in all subsequent study groups. These groups included treatment with NSD 1015 (general AADC inhibitor) or p-chlorophenylalanine (PCPA, inhibitor of tryptophan hydroxylase, TPH). In addition, the effect of a low-tryptophan (Trp) diet was investigated. NSD 1015 or Trp depletion did not affect any model parameters, but PCPA reduced [11C]5-HTP uptake, and the k_3. This was unexpected as NSD 1015 directly inhibits the enzyme converting [11C]5-HTP to [11C]5-HT, suggesting that trapping of radioactivity does not distinguish between parent tracer and its metabolites. As different results have been acquired in monkeys and humans, [11C]5-HTP-PET may be suitable for measuring 5-HT synthesis in primates, but not in rodents.

INTRODUCTION

The neurotransmitter serotonin, or 5-hydroxytryptamine (5-HT), is implied in several functions of the central nervous system, such as regulation of mood. Antidepressants, like selective serotonin reuptake inhibitors, increase the levels of serotonin in the synaptic cleft by blocking the serotonin transporter or by occupying the serotonin receptors. 5-HT synthesis may be an important aspect in the efficacy of antidepressants, as enough 5-HT should be produced for replenishing 5-HT stocks.[1–3]

Serotonin is produced by neurons, of which the cell bodies lie in the raphe nuclei and project to almost every region of the brain. Serotonin is synthesized from the amino acid tryptophan (Trp), mainly in synaptic endings. This process takes place in two enzymatic steps. First, Trp is converted to 5-hydroxytryptophan (5-HTP) by the enzyme tryptophan hydroxylase (TPH). Second, 5-HTP is converted to 5-HT by aromatic amino acid decarboxylase (AADC). 5-HT is transported into vesicles by the vesicular monoamine transporter. When serotonergic neurons fire, such vesicles fuse with the synaptic membrane to release 5-HT into the synaptic cleft. Released serotonin can be pumped back into the nerve endings by serotonin transporter, and can either be stored in the vesicles or be degraded by monoamine oxidase to 5-hydroxyindoleacetic acid (5-HIAA), which leaves the brain through the cerebrospinal fluid.

Besides activity of the enzymes involved in 5-HT synthesis, several other processes may influence the production of 5-HT. The availability of Trp for 5-HT production is the rate-limiting step in this metabolic pathway.[4,5] Trp is transported over the blood–brain barrier by the large neutral amino acid transporter (LAT). Transported Trp is not only used for 5-HT synthesis, but also incorporated into proteins and used for the production of kynurenine. The rate-limiting step in kynurenine production is the activity of the enzyme indoleamine 2,3-dioxygenase. Increased activity of indoleamine 2,3-dioxygenase may result in reduced availability of Trp for serotonin synthesis.[6]

As direct measurement of serotonin synthesis is difficult, indirect estimates are commonly employed. 5-HT turnover rates can be measured by determining 5-HIAA concentrations or the 5-HTP/5-HIAA ratio in cerebrospinal fluid.[7] However, this is an invasive method, as a lumbar puncture is necessary to obtain cerebrospinal fluid. Another method is measurement of the levels of 5-HT in blood platelets, as 5-HT is synthesized within these cells in a way similar to neurons. The validity of this procedure is questionable, for peripheral levels of 5-HT may not reflect corresponding levels in the brain.[8–10]

The only direct and non-invasive methods for measuring metabolic processes in the living brain are positron emission tomography (PET) and single-photon emission computed tomography. Several PET tracers have been produced for this purpose.[7] Radiolabeled Trp is not optimal, as Trp is also incorporated into proteins and used in the kynurenine pathway, rather than being used for 5-HT synthesis.[11] Tracer incorporation into proteins can be avoided by using a radiolabeled analog of Trp. Diksic and colleague's labeled α-methyltryptophan (AMT) with carbon-11.[12–17] However, AMT can still enter the kynurenine

[1]Department of Nuclear Medicine and Molecular Imaging, University of Groningen, University Medical Center Groningen, Groningen, The Netherlands and [2]Laboratory Medicine, University of Groningen, University Medical Center Groningen, Groningen, The Netherlands. Correspondence: Dr AKD Visser, University Medical Center, Nuclear Medicine and Molecular Imaging, Hanzeplein 1, Groningen 9700 RB, The Netherlands.
E-mail: visserakd@umcg.nl

pathway.[18,19] Consequently, [11C]AMT uptake reflects both 5-HT and kynurenine synthesis. Although some studies support the idea that [11C]AMT-PET measures 5-HT synthesis rates,[20] this may not be true under pathologic conditions, which are accompanied by neuroinflammation.

Another option to measure 5-HT synthesis with PET, is labeling the endogenous precursor of serotonin, [11C]5-HTP.[21,22] A great advantage of this compound is that it is metabolized exactly in the same way as endogenous 5-HTP. Several studies with [11C]5-HTP have indicated that this tracer can be used to measure 5-HT synthesis rates by kinetic modeling of PET data. The rate constant for accumulation of [11C]5-HTP, K_{acc}, calculated using a two-tissue compartment model (2TCM) with irreversible tracer trapping, reflects 5-HT synthesis rates.[23,24]

The trapping of radioactivity in the brain regions represents the production of [11C]5-HT and its metabolite [11C]5-HIAA. When the enzyme monoamine oxidase, converting 5-HT to 5-HIAA, is inhibited in monkeys, the trapping of radioactivity is unchanged.[24] This indicates that within a period of 60 minutes, there is no significant loss of radiolabeled metabolites from monkey brain, and the trapping of ^{11}C reflects 5-HT synthesis. Inhibition of AADC, and thus the conversion of 5-HTP to 5-HT, reduces the value of k_3, which suggests that this rate constant is closely related to the decarboxylation of [11C]5-HTP.[24]

Positron emission tomography studies with [11C]5-HTP have only been performed in monkeys or humans. To our knowledge, only one study applied [11C]5-HTP in rodents.[25] Rats were killed 40 minutes after [11C]5-HTP injection and radioactive metabolites in the striatum and cerebellum were determined by high-performance liquid chromatography. The results of this analysis raise the question whether pharmacologically induced changes of 5-HT synthesis in the rodent brain can be detected also with PET. If so, small animal imaging could be used to examine the mechanism of action of antidepressants.

The enzymatic steps in 5-HT synthesis can be inhibited by administering various drugs, thus one could investigate what [11C]5-HTP is exactly measuring. Levels of the precursor Trp can be reduced by feeding animals a special, Trp-free diet, lacking Trp but containing identical levels of other amino acids as the control diet. As Trp is the direct precursor of 5-HT, we expect a decrease of 5-HT synthesis in animals fed a Trp-free diet. The first enzymatic step in 5-HT synthesis, hydroxylation of Trp by TPH, can be inhibited by para-chlorophenylalanine (PCPA), which strongly reduces 5-HT content in the rat brain.[26] As PCPA treatment reduces the conversion from Trp to 5-HTP, 5-HT synthesis should decrease as well. The second step in 5-HT synthesis, decarboxylation of 5-HTP by AADC, can be inhibited in peripheral organs by carbidopa, without affecting AADC activity in the brain.[27] Treatment of animals with carbidopa should not influence cerebral rates of 5-HT synthesis, but only reduce the peripheral metabolism of 5-HTP. When peripheral metabolism of [11C]5-HTP is reduced, more parent tracer becomes available for uptake in the brain. A final compound, NSD 1015, inhibits AADC activity both in the brain and periphery.[28] Treatment of animals with NSD 1015 should decrease 5-HT synthesis rates in rat brain, as the production of 5-HT from 5-HTP is directly inhibited. An overview of the manipulations used in this study is presented in Figure 1.

Thus, we performed the current study that is aimed at answering the following questions: (1) Can [11C]5-HTP uptake in rat brain be increased by inhibiting peripheral AADC with carbidopa? (2) Can changes of 5-HT synthesis after pharmacologic inhibition of key enzymes be detected with [11C]5-HTP and microPET?

MATERIALS AND METHODS

Animals

Adult male Wistar rats (CpB:WU) weighing $317 \pm 34\,g$ were housed in pairs (Harlan, Boxmeer, The Netherlands). They were kept under a 12:12 hour
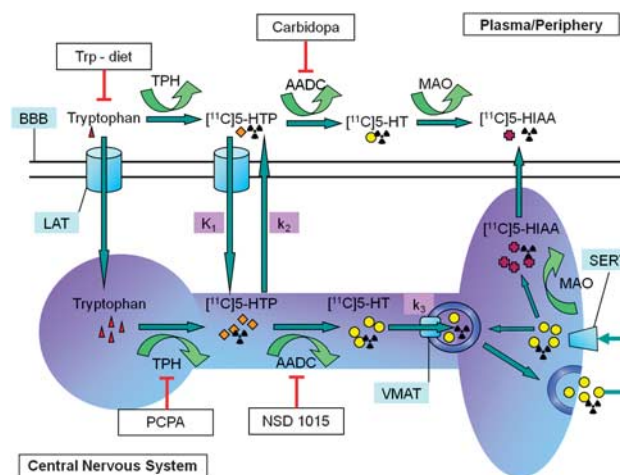
Figure 1. Manipulations in the serotonin synthesis pathway. Serotonin (5-HT) synthesis takes place within neurons in the brain and cells in the periphery. Tryptophan (Trp) is the amino acid precursor of 5-HT, which is transported by the large amino acid transporter (LAT) over the blood–brain barrier. Within the neuron, Trp is hydroxylated by tryptophan hydroxylase (TPH), the rate-limiting enzyme in the synthesis pathway, to 5-HTP. In turn, 5-HTP is decarboxylated to 5-HT by AADC. 5-HT is transported into vesicles by the vesicular monoamine transporter. When these vesicles fuse with the synaptic membrane, 5-HT is released in the synaptic cleft and can be taken up by the serotonin transporter. Finally, 5-HT is metabolized to 5-HIAA by monoamine oxidase and transported out of the brain. [11C]5-HTP follows the same pathway as endogenous 5-HTP. Different treatments can be used to manipulate different aspects of the 5-HT synthesis pathway. In this study, we used a Trp low diet (Trp − diet) to deplete rats from the 5-HT precursor. Carbidopa was used to inhibit peripheral AADC, and NSD 1015 was used to inhibit both peripheral and central AADC. Para-chlorophenylalanine (PCPA) was used to inhibit TPH. The different kinetic modeling rates are represented in purple. Adjusted from Visser et al.[7]

light:dark cycle (light on at 7.00 a.m.) with food and water available ad libitum. Animals were either fed a diet with $0.025\,g$ Trp/100 g (Trp depletion) or $0.25\,g$ Trp/100 g (Research Diet Services, The Netherlands, for 4 days). The animal experiments were performed by licensed investigators in compliance with the Law on Animal Experiments of The Netherlands. The protocol was approved by The Institutional Animal Care and Use Committee of the University of Groningen.

Tracer and Drug Treatment

[11C]5-HTP was produced according to a published method.[22] The average injected dose of [11C]5-HTP was 12.0 ± 6.4 MBq with a specific radioactivity of 23.4 ± 11.2 GBq/μmol. All drugs were administered by i.p. injection. Carbidopa was dissolved in water (1 mg/mL or 2.5 mg/mL), and doses of 1 or 10 mg/kg were administered 1 hours before tracer injection. NSD 1015 was dissolved in saline at 100 mg/mL, and a dose of 100 mg/kg was administered 30 minutes before tracer injection. Para-chlorophenyl-alanine (PCPA) was dissolved in saline at 150 mg/mL and a single dose of 150 mg/kg was administered on the two consecutive days before PET scanning. The second PCPA administration took place 24 hours before tracer injection.

In the initial part of this project, the dose-dependent effect of carbidopa was examined by treating groups of animals with 0, 1 or 10 mg/kg carbidopa. In the second part of the study, all animals were treated with 10 mg/kg carbidopa. Separate groups of animals were used for metabolite analysis.

MicroPET Acquisition and Image Reconstruction

Animals were anesthetized with isoflurane (5% in medical air for induction, 2% for maintenance). A cannula was placed in the left femoral artery to

enable arterial blood sampling during PET scanning. Two cannulated animals were positioned in the Siemens/Concorde MicroPET Focus220 camera, with the brain in the field-of-view. A 515second-transmission scan with a ^{57}Co source was made, to allow correction of the PET images for attenuation and scatter. Tracer solution was injected through the penile vein. MicroPET data was acquired, using a list mode protocol of 96 minutes. The camera was started at the moment of injection of the first animal, whereas the second animal was injected after 6 minutes. During microPET scanning, 15 arterial blood samples (volume 0.1 to 0.15 mL) were drawn at different time-points: 15, 30, 45, 60, 75, and 90 seconds; 2, 3, 5, 7.5, 10, 15, 30, 60, and 90 minutes. The 15 blood samples for determination of input curves were centrifuged for 5 minutes at 13,000 rpm. Plasma was collected (25 μL) and radioactivity was measured in a calibrated γ-counter.

List mode data were reframed into 8 frames of 30 seconds, 3 of 60 seconds, 2 of 120 seconds, 2 of 180 seconds, 3 of 300 seconds, 3 of 600 seconds, 1 of 720 seconds, and 1 of 960 seconds. Data of each frame were reconstructed employing an iterative algorithm (OSEM2D with Fourier rebinning, 4 iterations, and 16 subsets). The final data sets consisted of 95 slices with a thickness of 0.8 mm and an in-plane image matrix of 128×128 pixels. Voxel size was 0.5 mm $\times$ 0.5 mm $\times$ 0.8 mm. Linear resolution of the images at the center of the field-of-view was $\sim$ 1.5 mm.

Ex vivo Biodistribution

After scanning, animals were killed by extirpation of the heart under deep isoflurane anesthesia and blood was collected. The blood was centrifuged for 10 minutes at 6,000 rpm, and plasma and a cell fraction were collected separately. Samples of different tissues were taken and weighed. Radioactivity in all samples was measured in a γ-counter. Standard uptake values (SUV) were calculated using the formula:

$$\frac{\text{Tissue activity } (MBq/g)}{(\text{Injected dose } (MBq)/\text{Bodyweight } (g))}.$$

The following brain regions were dissected: bulbi olfactorii, hippocampus, striatum, cortex, pons, medulla, cerebellum, and the rest of the brain.

Tryptophan Concentration

Blood samples were taken after extirpation of the heart, and plasma was collected as mentioned above. Approximately 0.3 mL of plasma was pipetted on an Amicon ultrafilter with 25 kDa cut-off. Free and bound Trp were separated by 30 minutes of centrifugation at 3,000 rpm. The ultrafiltrate was frozen (-20°C) to determine free Trp at a later moment. A sample of unfiltered plasma was used to assess total Trp. Free and total Trp were measured as described previously.[29]

Metabolite Analysis

In separate groups, blood samples (0.8 to 1.5 mL) were drawn for metabolite analysis at 5, 10, 20, 40, and 60 minutes after tracer injection. The blood was centrifuged (2 minutes at 13,000 rpm). Plasma was collected and 5% perchloric acid was added. After Vortex mixing, proteins were removed by 2 minutes of centrifugation at 13,000 rpm. The supernatant was analyzed by high-performance liquid chromatography, using an X-Terra C18-column (Waters, 4.6 $\times$ 250 mm). The high-performance liquid chromatograph was equipped with a UV detector (set at 254 nm). Parent [^{11}C]5-HTP was separated from radioactive metabolites using gradient elution (buffer A: 50 mmol/L potassium dihydrogen phosphate, pH 3.3, buffer B: 30% acetonitrile in buffer A). The gradient was programmed as follows: 0 to 2 minutes 90% A and 10% B; 2 to 10 minutes 60% A and 40% B; 10 to 10.1 minutes 0% A and 100% B; 10.1 to 15 minutes 0% A and 100% B; 15 to 15.1 minutes 90% A and 10% B; 15.1 to 17 minutes 90% A and 10% B. Flow rate was 1 mL/minute and the gradient was linear.

The eluate was collected by a fraction collector, every 30 seconds and every 20 seconds during peak collection, and measured in a γ-counter. Fractions of parent tracer and metabolites were calculated from the radiochromatograms.

MicroPET Data Analysis

A volume of interest of the whole brain was drawn on a template of the rat brain (rat scanned with [^{11}C]verapamil and treated with cyclosporine). Positron emission tomography images were re-aligned to this template, and the volume of interest was used to calculate time–activity curves (TACs). Model fits to these TACs were performed using in-house MatLab software. Using metabolite-corrected plasma data as input function, a one-tissue compartment model or a 2TCM with irreversible tracer trapping were applied to fit the TACs. Blood volume was fixed to 3.6%.[30]

Only the first 62 minutes of the scans were analyzed. As Patlak analysis requires an equilibrium state, which is reached after 20 minutes, a 40 minutes data set is too short. When a longer (90 minutes) data set was used, there is a higher chance of washout of [^{11}C]5-HIAA from the brain. We therefore used 62 minutes of data. The accumulation constant, K_{acc}, was calculated with the formula:

$$K_{acc} = \frac{K_1 * k_3}{k_2 + k_3}$$

A Patlak plot of the data was also made, as this graphical method can also be used to estimate the accumulation constant independent of the specific trapping model.[31,32]

Statistical Analysis

For analysis of TACs, metabolite curves, and plasma curves, repeated measures analysis of variance (ANOVA) with Bonferroni posttest were used. One-way ANOVA was used for comparison of the values of K_1, k_2, k_3, K_{acc}, and Patlak constant in the different groups. Dunnett's multiple comparison tests were applied for further analysis of group differences. Correlations between the Patlak constant and K_{acc} were examined by Spearman rank correlation. As we expected to observe a decrease in Trp levels in animals exposed to a low-Trp diet, measured plasma–Trp concentrations in the control and Trp depleted groups were directly compared using Student's t-test. The Akaike criterion of one-tissue compartment model and 2TCM were compared by a paired t-test, where we expect a better fit of the 2TCM. All statistical analysis was performed with GraphPad Prism 5 (GraphPad Software, La Jolla, CA, USA).

RESULTS

Tryptophan Depletion

Direct comparison of the Trp depleted ($N = 9$) and control group ($N = 12$) indicated no significant change of total Trp, but there was a significant decrease of free Trp (-28.5%) in plasma of animals that had been fed a low-Trp diet (t-test, $t = 2.636$, $Df = 19$, $P = 0.016$). One-way ANOVA showed a significant effect of treatment on total Trp levels (control, NSD, PCPA, and Trp low diet) ($F = 4.64$, $Df = 3$, $P = 0.009$). A significant decrease in total Trp levels (-24%) occurred in animals treated with PCPA (Dunnett's multiple comparison, $q = 2.99$, $P < 0.05$). The other treatments did not affect either total or free Trp. Neither total nor free levels of Trp were correlated with K_{acc}.

Metabolite Analysis

For all groups, metabolite analysis was performed. There was a significant difference in metabolism between the different treatment groups (repeated measures ANOVA, $F = 93.74$, $Df = 5$, $P < 0.0001$). After Bonferroni posttests, it appeared that 10 mg/kg carbidopa decreased metabolism (also in combination with the other treatments).

After metabolite correction, there was a significant difference between plasma curves (repeated measures ANOVA, $F = 9.96$, $Df = 5$, $P < 0.0001$). After Bonferroni posttest, it appeared that this significant difference was present between almost all treatment groups, but only in the early time-points of the plasma peak. See Figure 2 for metabolite and metabolite-corrected plasma curves.

Tracer Uptake

As visual inspection of microPET images and biodistribution data indicated a homogeneous uptake of [^{11}C]5-HTP in rat brain, we used TACs of whole brain ROIs for kinetic modeling.

Time–activity curves of whole brain of animals treated with different carbidopa concentrations were significantly different (repeated measures ANOVA, interaction, $F = 2.4$, $Df = 40$, $P < 0.0001$). After Bonferroni correction, an increase in [^{11}C]5-HTP

uptake was observed between animals treated with 0 mg/kg and 10 mg/kg carbidopa (Figure 3A).

Biodistribution data also indicated a significant increase of tracer SUV in the brain after carbidopa treatment (2-way ANOVA, $F = 49.89$, $Df = 2$, $P < 0.0001$). Comparison of the different doses with Bonferroni posttests revealed that the SUV in the cortex was increased in animals treated with 1 mg/kg carbidopa, as compared with untreated controls, with an average SUV of 0.48 ± 0.07 for animals treated with 1 mg/kg carbidopa versus 0.15 ± 0.02 for untreated animals. Trends towards an increase were also seen in the hippocampus, cerebellum, pons, medulla, and the rest of the brain. At the higher dose used (10 mg/kg), carbidopa increased tracer uptake in all studied brain regions, although the change in striatum and hippocampus did not reach statistical significance (Figure 4A). As the effect of carbidopa appeared to be dose-dependent, we used 10 mg/kg carbidopa in all subsequent experiments to increase tracer delivery to the brain.

Brain TACs indicated no significant difference in [^{11}C]5-HTP uptake in animals treated with 10 mg/kg carbidopa or the combination of 10 mg/kg carbidopa with either NSD, PCPA, or a Trp low diet (repeated measures ANOVA, $F = 0.45$, $Df = 2$, $P = 0.72$) (Figure 3B). Biodistribution did indicate a significant decrease in tracer uptake after the different treatments (two-way ANOVA, $F = 20.25$, $Df = 3$, $P < 0.0001$). Bonferroni posttest revealed a significant difference in the PCPA-treated group, in the hippocampus and medulla, and a trend towards a decrease in all the other brain regions investigated. NSD 1015 and a low-Trp diet did not affect brain uptake of [^{11}C]5-HTP (Figure 4B).

Analysis of tracer uptake in the peripheral organs indicated a significant increase of radioactivity due to carbidopa treatment (two-way ANOVA, $F = 4.73$, $Df = 2$, $P = 0.0095$). Bonferroni posttest

revealed an increased radioactivity in the urine after treatment of animals with 1 mg/kg carbidopa, although a large individual variation was observed. The higher dose of 10 mg/kg had the opposite effect, as the amount of radioactivity in the urine was tremendously reduced. Carbidopa did not affect tracer uptake in any of the other organs, although uptake in the red blood cells and pancreas tended to be increased after treatment with 10 mg/kg carbidopa, compared with untreated controls (Figure 4C).

Para-chlorophenylalanine reduced [^{11}C]5-HTP uptake in the pancreas and increased radioactivity in the kidney and urine (two-way ANOVA, $F = 13.49$, $Df = 3$, $P < 0.0001$). Feeding rats a low-Trp diet also increased tracer elimination via the renal route (Figure 4D).

Kinetic Modeling

A 2TCM fitted whole brain TACs better than a one-tissue compartment model, as shown by lower values of the Akaike criterion (AICc corrected for small sample size; paired t-test, $t = 9.07$, $Df = 46$, $P < 0.0001$), although both fits were good with an average Akaike value of 239 ± 1.8 for the one-tissue compartment model and 225 ± 2.6 for the 2TCM. Cerebral blood volume was fixed at 3.6% in kinetic modeling, to avoid model fits with physiologically irrelevant high values ($>10\%$) for blood volume. In some cases, fixing the blood volume also resulted in a visually better fit.

Calculated values for the Patlak rate constant correlated well with K_{acc} ($r = 0.733$, $P = 0.0001$), therefore only K_{acc} is presented in Figure 5. Data analysis with one-way ANOVA revealed that carbidopa treatment did not result in significant changes in K_{acc}
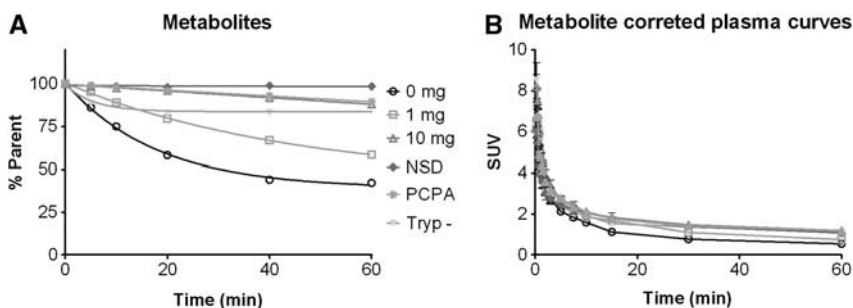
Figure 2. Metabolism in plasma of all different groups (**A**) and metabolite-corrected time–activity plasma curves (**B**). Data are depicted as mean ± s.e.m. (**A**) Especially, the different doses of carbidopa significantly affect metabolism of [^{11}C]5-HTP in plasma. (**B**) Metabolite-corrected plasma–input curves only significantly differ in some of the first few time-points.
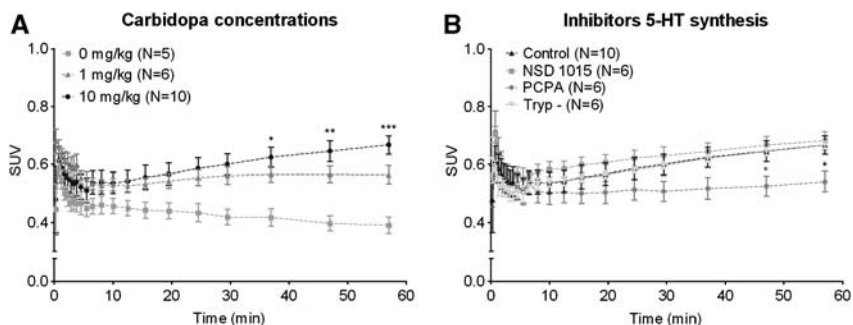
Figure 3. Time–activity curves of different concentrations of carbidopa (**A**) and the different enzymatic inhibitors (**B**). Time–activity curves were obtained from positron emission tomography (PET) images by drawing a region of interest (ROI) of the whole brain. Data are depicted as mean ± s.e.m. (**A**) Both 1 mg/kg and 10 mg/kg increase the uptake of [^{11}C]5-HTP over time, although this is only significant for the 10 mg/kg dose. (**B**) Only para-chlorophenylalanine (PCPA) had an effect on tracer uptake of [^{11}C]5-HTP over time, compared with control (10 mg/kg carbidopa). SUV, standard uptake values. $*P < 0.05$; $**P < 0.01$; $***P < 0.001$.
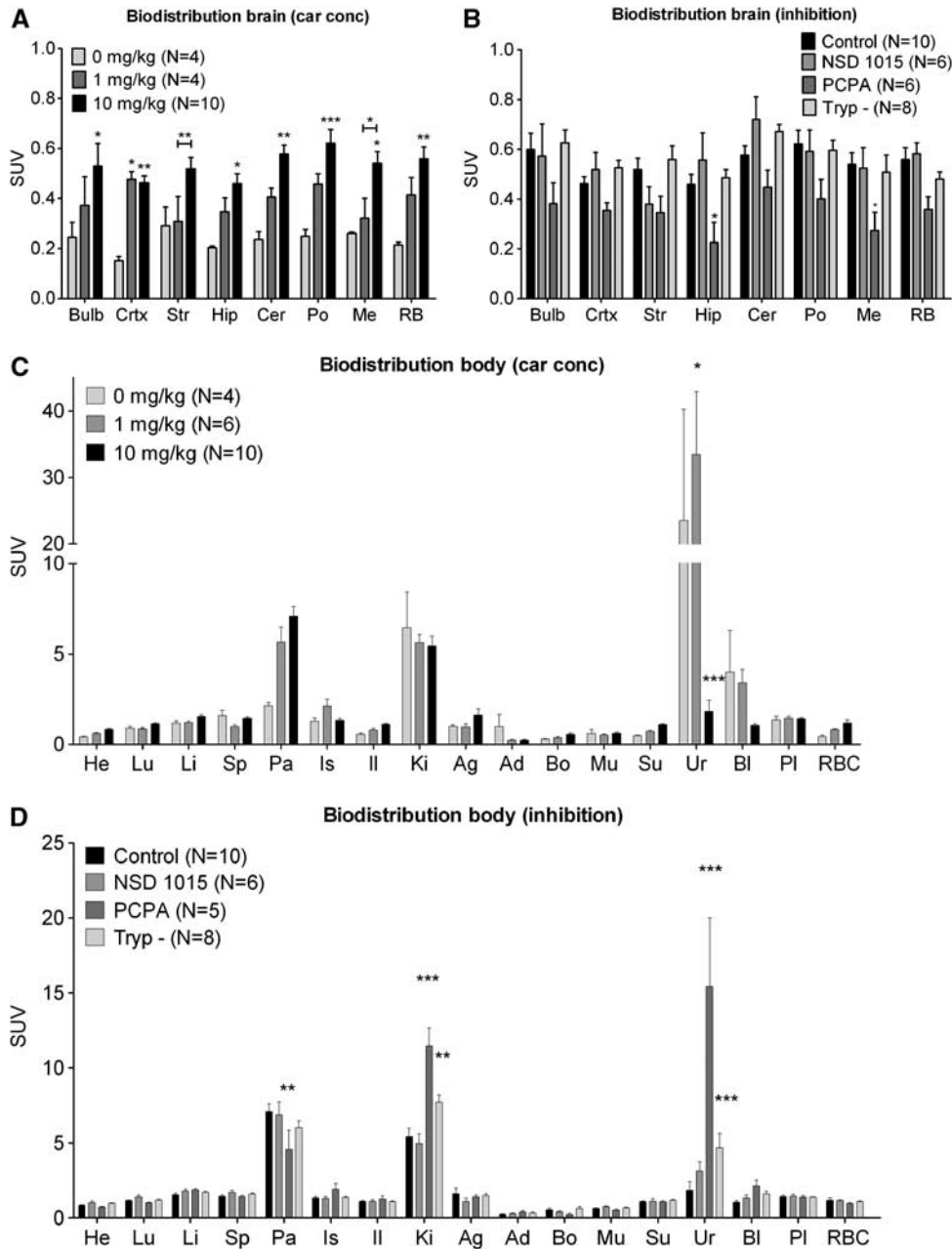
Figure 4. Biodistribution data for brain regions (**A** and **B**) and peripheral organs (**C** and **D**) after carbidopa treatment or enzymatic inhibition. After scanning, animals were killed and different organs were collected for analysis in the γ-counter. Data are depicted as mean ± s.e.m. (**A**) 10 mg/kg carbidopa increased the uptake of [¹¹C]5-HTP in almost all brain regions, whereas 1 mg/kg only increased the uptake in the cortex. (**B**) Inhibition of TPH by PCPA decreased the uptake of [¹¹C]5-HTP in the hippocampus and medulla. (**C**) 1 mg/kg carbidopa increased excretion of radiolabeled compounds through the urine, while a 10 mg/kg dose largely decreased excretion of these compounds. There is also high uptake of [¹¹C]5-HTP in the pancreas, which tends to increase by treatment with carbidopa. (**D**) Inhibition of TPH by PCPA decreases uptake of [¹¹C]5-HTP in the pancreas and increased uptake in the kidney and urine. Tryptophan (Trp) depletion also increased the uptake in the kidney and urine. Abbreviations A/B: Bulb, bulbus olfactorii; Crtx, cortex; Str, striatum, Hip, hippocampus; Cer, cerebellum; Po, pons; Me, medulla; RB, rest brain. Abbreviations C/D: He, heart; Lu, lung; Li, liver; Sp, spleen; Pa, pancreas; Is, intestine small; Il, Intestine large; Ki, kidney; Ag, adrenal gland; Ad, adipose tissue; Bo, bone; Mu, muscle; Su, submandibular gland; Ur, urine; Bl, bladder; Pl, plasma; RBC, red blood cells. *$P < 0.05$; **$P < 0.01$; ***$P < 0.001$.

$(F = 0.13, Df = 2, P = 0.88)$ (Figure 5A). NSD 1015, PCPA, and Trp depletion did not result in significant changes of K_{acc} either, although a trend towards a decrease was seen after 2 days of treatment with PCPA (one-way ANOVA, $F = 2.76, Df = 3, P = 0.0655$).

Inter-individual variation of K_1 and K_2 was high in all groups, but values for k_3 were more stable. As this rate constant possibly reflects the enzymatic activity of AADC, it is of equally great interest as K_{acc}. There was no significant effect of carbidopa treatment on k_3 (one-way ANOVA, $F = 0.9767, Df = 2, P = 0.40$) (Figure 5C). There was a significant effect of other treatments on k_3 (one-way ANOVA, $F = 3.26, Df = 3, P = 0.04$), attributable to a reduction in k_3 after PCPA treatment (Dunnet's multiple comparison, $q = 2.70, P < 0.05$) (Figure 5D). None of the other constants
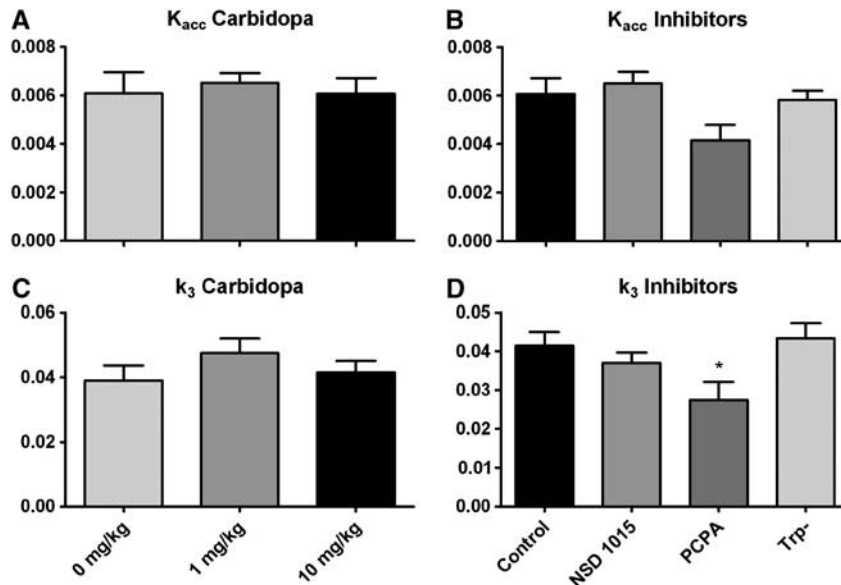
Figure 5. Rate constants after treatments with different doses of carbidopa (**A** and **C**) or different enzymatic inhibitors (**B** and **D**). Time–activity curves and plasma–input curves were fitted in a two-tissue compartment model (2TCM), rendering K_{acc} and k_3. Data are depicted as mean ± s.e.m. (**A**) Carbidopa does not influence K_{acc}. (**B**) There is no significant effect of inhibition of tryptophan hydroxylase (TPH) by para-chlorophenylalanine (PCPA), aromatic amino acid decarboxylase (AADC) by NSD 1015, or Trp depletion on K_{acc}, although a trend towards a decrease is seen after PCPA treatment. (**C**) Carbidopa does not influence k_3. (**D**) Only PCPA decreases k_3 significantly. *$P < 0.05$.

Table 1. Summary of parameters determined with kinetic modeling

	K_1	k_2	k_3	K_{acc}	Patlak	AICc	C_{Trp} tot (μmol/L)	C_{Trp} free (μmol/L)
0 mg/kg car	0.37 ± 0.51	2.61 ± 3.95	0.04 ± 0.01	0.006 ± 0.002	0.003 ± 0.001	220 ± 5.59	56.3 ± 13.4	17.7 ± 3.51
1 mg/kg car	0.70 ± 0.41	4.58 ± 4.07	0.05 ± 0.01	0.007 ± 0.001	0.005 ± 0.001	228 ± 5.54	61.9 ± 4.89	21.3 ± 6.80
10 mg/kg car (control)	0.27 ± 0.36	1.75 ± 2.22	0.04 ± 0.01	0.006 ± 0.002	0.004 ± 0.001	229 ± 24.4	56.6 ± 8.67	17.7 ± 4.10
NSD 1015	0.16 ± 0.07	0.88 ± 0.42	0.04 ± 0.007	0.006 ± 0.001	0.004 ± 0.002	238 ± 5.87	55.4 ± 10.6	16.5 ± 3.05
PCPA	0.42 ± 0.40	2.69 ± 2.65	0.03 ± 0.01[a]	0.004 ± 0.002	0.003 ± 0.001	222 ± 11.5	41.3 ± 7.38[a]	15.7 ± 4.02
Trp-	0.12 ± 0.07	0.88 ± 0.65	0.04 ± 0.01	0.006 ± 0.001	0.004 ± 0.001	213 ± 14.6	57.1 ± 7.54	13.3 ± 2.69[b]

Abbreviation: car, carbidopa.
K_1, k_2, k_3 and K_{acc} are determined by a two-tissue compartment model with irreversible tracer trapping. In addition, the Patlak value, Akaike criterion (AICc), and total (C_{Trp} tot) and unbound (free, C_{Trp} free) tryptophan concentrations are shown. Data are depicted as mean ± SD. [a]Comparison of NSD 1015, PCPA and Trp- to controls, $P < 0.05$. [b]Direct comparison of Trp- to controls, $P < 0.05$.

(K_1 or K_2) showed significant difference between groups, which is probably caused by the high variability between individual animals. The kinetic modeling data are summarized in Table 1.

DISCUSSION

This study focused on two questions: (1) whether carbidopa can dose-dependently increase [^{11}C]5-HTP uptake in rat brain, and (2) whether enzyme inhibitors or Trp depletion affect [^{11}C]5-HTP trapping in the rat brain. As [^{11}C]5-HTP is metabolized in exactly the same way as endogenous 5-HTP and [^{11}C]5-HIAA is the main radiolabeled metabolite contributing to the cerebral signal after 40 to 60 minutes, trapping of [^{11}C]5-HTP should reflect the rate of 5-HT synthesis.[25]

Both the microPET and biodistribution data indicate that carbidopa increases brain uptake (SUV) in a dose-dependent way, with the greatest effect occurring at a dose of 10 mg/kg. Increased tracer uptake in the brain could result from a decrease in the peripheral breakdown of [^{11}C]5-HTP. The reduction of urinary radioactivity after carbidopa treatment, indicating decreased tracer excretion, confirmed this hypothesis. Carbidopa treatment does not influence K_{acc} or k_3, indicating that AADC

activity in the brain is the same as under control conditions. Therefore, we used 10 mg/kg carbidopa in all other treatment groups.

We expected to observe a large reduction of [^{11}C]5-HTP trapping after inhibition of AADC in the brain with NSD, as this enzyme converts [^{11}C]5-HTP to [^{11}C]5-HT. Surprisingly, 100 mg/kg of NSD had no significant effect on tracer trapping. After inhibition of AADC with NSD, the total uptake of radioactivity may not be altered, because of the fact that PET cannot distinguish between [^{11}C]5-HT and [^{11}C]5-HTP. In order to see differences in k_3 or K_{acc}, [^{11}C]5-HTP should exit the brain and not be trapped. Such trapping was in fact measured in rat brain by Lindner *et al.*[25] In a study with [^{11}C]5-HTP in monkeys, the brain uptake of radioactivity was even increased after administration of NSD 1015, although a decrease in K_{acc} was observed.[33] The observed increase of radioactivity in monkey brain could be due to inhibition of peripheral AADC by NSD 1015, an effect which we also observed in rats after carbidopa treatment. There seems to be a species difference between monkeys and rats, where the k_3 in monkeys is influenced by NSD 1015 and in rats, it is not.

Besides NSD 1015, we examined the effect of PCPA, an inhibitor of the enzyme TPH, which is located upstream in the 5-HT

synthesis pathway. Surprisingly, PCPA had a significant effect on TACs calculated from the microPET data and SUV values from the biodistribution study. Tryptophan hydroxylase inhibition additionally decreased k_3, and tended to decrease K_{acc}. As neither [^{11}C]5-HTP nor [^{11}C]5-HT are a substrate for TPH, these were surprising findings. Decreases in SUV and k_3 in the brain coincided with a decrease of the levels of total Trp in plasma, although Trp levels were not correlated with any of these values. The most likely explanation is that PCPA competes with [^{11}C]5-HTP for transport over the blood–brain barrier. Competition at the level of LAT is highly probable, as PCPA has been shown to compete with Trp for blood–brain barrier transport.[34] However, this competition should influence the K_1 (and thus K_{acc}), but not the decarboxylase activity rate constant of AADC (k_3). Another explanation is that reduced 5-HT synthesis (by inhibition of the rate-limiting enzyme TPH) also influences enzymatic activity more downstream, e.g. AADC activity.

Trp depletion did not affect the brain uptake of [^{11}C]5-HTP, although it increased tracer excretion via the renal route. We expected to see a decrease in the levels of total and free (unbound) Trp in plasma, but only the free fraction was found to show a decline. The relatively minor effect of the low-Trp diet on plasma levels of free Trp explains why we could not measure any effect on serotonin synthesis rates in the brain.

An interesting observation in biodistribution studies was the high specific trapping of radioactivity in the pancreas. This may be physiologically meaningful, because 5-HT regulates insulin secretion by β-cells in the islets of Langerhans.[35] Indeed, both in vitro and in vivo studies of our laboratory have shown that serotonin synthesis and trapping of [^{11}C]5-HTP and its metabolites in rat pancreas are specific to the β-cells compared with exocrine cells.[36] So this may be an interesting finding for future studies on imaging of pancreatic β-cells.

In summary, almost all results indicate that assessment of the validity to use [^{11}C]5-HTP-PET as a measure for 5-HT synthesis rates in rat failed to convincingly show alterations in response to various interventions. Drug effects on enzyme and transport activities in the metabolic pathway of [^{11}C]5-HTP cannot always be distinguished, probably causing the aforementioned problem. Kinetic modeling is based on a mathematical approximation, and it may be hard to relate individual k values to a physiologic process. A simplified model, like the 2TCM, may pool multiple metabolic steps into a single mathematical compartment and the data presented here does not allow us to accurately decompose this process. This is probably also the reason why Lindner et al.[25] could find a difference in k_3 after NSD 1015 treatment, as they quantified all the different metabolites of [^{11}C]5-HTP post mortem, in brain homogenates. Thus, they knew exactly how much radioactivity belonged to a certain compartment of the kinetic model. A PET camera cannot distinguish different radioactive species, and although K_4 seems negligible, other processes like transport and retention of unmetabolized [^{11}C]5-HTP could influence the model parameters. Eventually, this may lead to ambiguity of the individual k values. A major source of variation may be the low uptake of [^{11}C]5-HTP in rat brain.

Although our data indicate that [^{11}C]5-HTP is not useful for measuring serotonin synthesis in rat brain, the tracer may be useful in primates, as inhibitors of central AADC reduce the measured values of k_3 and K_{acc} in monkeys.[33]

CONCLUSION

Further validation of [^{11}C]5-HTP for measurement of 5-HT synthesis rates in human brain is definitely of great interest, especially for evaluation of 5-HT synthesis rates in patients with major depression. But based on our current data, [^{11}C]5-HTP and microPET are not suitable for pharmacodynamic studies in the rodent brain.

REFERENCES

1 Bosker FJ, Cremers TI, Jongsma ME, Westerink BH, Wikstrom HV, Den Boer JA. Acute and chronic effects of citalopram on postsynaptic 5-hydroxytryptamine(1A) receptor-mediated feedback: a microdialysis study in the amygdala. J Neurochem 2001; 76: 1645–1653.

2 Frey BN, Rosa-Neto P, Lubarsky S, Diksic M. Correlation between serotonin synthesis and 5-HT1A receptor binding in the living human brain: a combined alpha-[11C]MT and [18F]MPPF positron emission tomography study. Neuroimage 2008; 42: 850–785.

3 Okazawa H, Yamane F, Blier P, Diksic M. Effects of acute and chronic administration of the serotonin1A agonist buspirone on serotonin synthesis in the rat brain. J Neurochem 1999; 72: 2022–2031.

4 Evans AK, Reinders N, Ashford KA, Christie IN, Wakerley JB, Lowry CA. Evidence for serotonin synthesis-dependent regulation of in vitro neuronal firing rates in the midbrain raphe complex. Eur J Pharmacol 2008; 590: 136–149.

5 Fernstrom JD, Wurtman RJ. Brain serotonin content: physiological dependence on plasma tryptophan levels. Science 1971; 173: 149–512.

6 Dantzer R, O'Connor JC, Freund GG, Johnson RW, Kelley KW. From inflammation to sickness and depression: when the immune system subjugates the brain. Nat Rev Neurosci 2008; 9: 46–56.

7 Visser AK, Van Waarde A, Willemsen AT, Bosker FJ, Luiten PG, Den Boer JA et al. Measuring serotonin synthesis: from conventional methods to PET tracers and their (pre)clinical implications. Eur J Nucl Med Mol Imaging 2010; 38: 576–591.

8 Bianchi M, Moser C, Lazzarini C, Vecchiato E, Crespi F. Forced swimming test and fluoxetine treatment: in vivo evidence that peripheral 5-HT in rat platelet-rich plasma mirrors cerebral extracellular 5-HT levels, whilst 5-HT in isolated platelets mirrors neuronal 5-HT changes. Exp Brain Res 2002; 143: 191–197.

9 Janusonis S, Anderson GM, Shifrovich I, Rakic P. Ontogeny of brain and blood serotonin levels in 5-HT receptor knockout mice: potential relevance to the neurobiology of autism. J Neurochem 2006; 99: 1019–1031.

10 Sneddon JM. Blood platelets as a model for monoamine-containing neurones. Prog Neurobiol 1973; 1: 151–198.

11 Tracqui P, Morot-Gaudry Y, Staub JF, Brezillon P, Perault-Staub AM, Bourgoin S et al. Model of brain serotonin metabolism. II. Physiological interpretation. Am J Physiol 1983; 244: R206–R215.

12 Chugani DC, Chugani HT. PET: mapping of serotonin synthesis. Adv Neurol 2000; 83: 165–171.

13 Chugani DC, Muzik O, Chakraborty P, Mangner T, Chugani HT. Human brain serotonin synthesis capacity measured in vivo with alpha-[C-11]methyl-L-tryptophan. Synapse 1998; 28: 33–43.

14 Diksic M, Nagahiro S, Sourkes TL, Yamamoto YL. A new method to measure brain serotonin synthesis in vivo. I. Theory and basic data for a biological model. J Cereb Blood Flow Metab 1990; 10: 1–12.

15 Diksic M. alpha-Methyl tryptophan as a tracer for in vivo studies of brain serotonin system, from autoradiography to positron emission tomography. J Chem Neuroanat 1992; 5: 349–354.

16 Diksic M, Young SN. Study of the brain serotonergic system with labeled alpha-methyl-L-tryptophan. J Neurochem 2001; 78: 1185–1200.

17 Diksic M. Labelled alpha-methyl-L-tryptophan as a tracer for the study of the brain serotonergic system. J Psychiatry Neurosci 2001; 26: 293–303.

18 Batista CE, Juhasz C, Muzik O, Kupsky WJ, Barger G, Chugani HT et al. Imaging correlates of differential expression of indoleamine 2,3-dioxygenase in human brain tumors. Mol Imaging Biol 2009; 11: 460–466.

19 Chugani DC, Muzik O. Alpha[C-11]methyl-L-tryptophan PET maps brain serotonin synthesis and kynurenine pathway metabolism. J Cereb Blood Flow Metab 2000; 20: 2–9.

20 Cohen Z, Tsuiki K, Takada A, Beaudet A, Diksic M, Hamel E. In vivo-synthesized radioactively labelled alpha-methyl serotonin as a selective tracer for visualization of brain serotonin neurons. Synapse 1995; 21: 21–28.

21 Bjurling P, Watanabe Y, Tokushige M, Oda T, Långström B. Syntheses of -11C-labelled L-tryptophan and 5-hydroxy-L-tryptophan using a multi-enzymatic reaction route. J Chem Soc, Perkin Trans 1989: 1331–1334.

22 Neels OC, Jager PL, Koopmans KP, Eriks E, de Vries EGE, Kema IP et al. Development of a reliable remote-controlled synthesis of beta-[C-11]-5-hydroxy-L-tryptophan on a Zymark robotic system. J Labelled CompRadiopharm 2006; 49: 889–895.

23 Hagberg GE, Torstenson R, Marteinsdottir I, Fredrikson M, Langstrom B, Blomqvist G. Kinetic compartment modeling of [11C]-5-hydroxy-L-tryptophan for positron emission tomography assessment of serotonin synthesis in human brain. J Cereb Blood Flow Metab 2002; 22: 1352–1366.

24 Hartvig P, Lindner KJ, Tedroff J, Andersson Y, Bjurling P, Langstrom B. Brain kinetics of 11C-labelled L-tryptophan and 5-hydroxy-L-tryptophan in the rhesus monkey. A study using positron emission tomography. J Neural Transm Gen Sect 1992; 88: 1–10.

25 Lindner KJ, Hartvig P, Bjurling P, Fasth KJ, Westerberg G, Langstrom B. Determination of 5-hydroxy-L-[beta-11C]tryptophan and its in vivo-formed radiolabeled metabolites in brain tissue using high performance liquid chromatography: a study supporting radiotracer kinetics obtained with positron emission tomography. Nucl Med Biol 1997; 24: 733–738.

26 Koe BK, Weissman A. p-Chlorophenylalanine: a specific depletor of brain serotonin. J Pharmacol Exp Ther 1966; 154: 499–516.

27 Komai T, Kawai K, Nambu K, Miyakoshi N, Shindo H. Effect of carbidopa (MK-486) on the metabolic fate of L-3,4-dihydroxyphenylalanine (L-DOPA). I. Effect of carbidopa on the tissue DOPA decarboxylase and on the L-DOPA-2-¹⁴C uptake by the brain in rats. J Pharm.Dyn 1978; 1: 271–280.

28 Carlsson A, Lindqvist M. Dependence of 5-HT and catecholamine synthesis on concentrations of precursor amino-acids in rat brain. Naunyn Schmiedebergs Arch Pharmacol 1978; 303: 157–164.

29 Kema IP, Meijer WG, Meiborg G, Ooms B, Willemse PH, de Vries EG. Profiling of tryptophan-related plasma indoles in patients with carcinoid tumors by automated, on-line, solid-phase extraction and HPLC with fluorescence detection. Clin Chem 2001; 47: 1811–1820.

30 Julien-Dolbec C, Tropres I, Montigon O, Reutenauer H, Ziegler A, Decorps M et al. Regional response of cerebral blood volume to graded hypoxic hypoxia in rat brain. Br J Anaesth 2002; 89: 287–293.

31 Patlak CS, Blasberg RG, Fenstermacher JD. Graphical evaluation of blood-to-brain transfer constants from multiple-time uptake data. J Cereb Blood Flow Metab 1983; 3: 1–7.

32 Patlak CS, Blasberg RG. Graphical evaluation of blood-to-brain transfer constants from multiple-time uptake data. Generalizations. J Cereb Blood Flow Metab 1985; 5: 584–590.

33 Lundquist P, Blomquist G, Hartvig P, Hagberg GE, Torstenson R, Hammarlund-Udenaes M et al. Validation studies on the 5-hydroxy-L-[beta-11C]-tryptophan/PET method for probing the decarboxylase step in serotonin synthesis. Synapse 2006; 59: 521–531.

34 Knapp S, Mandell AJ. Parachlorophenylalanine--its three phase sequence of interactions with the two forms of brain tryptophan hydroxylase. Life Sci I 1972; 11: 761–771.

35 Paulmann N, Grohmann M, Voigt JP, Bert B, Vowinckel J, Bader M et al. Intracellular serotonin modulates insulin secretion from pancreatic beta-cells by protein serotonylation. PLoS Biol 2009; 7: e1000229.

36 Di Gialleonardo V, Signore A, Scheerstra EA, Visser AK, van Waarde A, Dierckx RA et al. 11C-hydroxytryptophan uptake and metabolism in endocrine and exocrine pancreas. J Nucl Med 2012; 53: 1755–1763.